

Aqueous Solubility of Piperazine and 2-Amino-2-methyl-1-propanol plus Their Mixtures Using an Improved Freezing-Point Depression Method

Philip Loldrup Fosbøl,* Randi Neerup, Muhammad Waseem Arshad, Zacarias Tecle, and Kaj Thomsen

Department of Chemical and Biochemical Engineering, Center for Energy Resources Engineering (CERE), Technical University of Denmark (DTU), Søtofts Plads, Building 229, DK-2800 Kongens Lyngby, Denmark

ABSTRACT: In this work the solid–liquid equilibrium (SLE) and freezing-point depression (FPD) in the electrolytic binary aqueous systems piperazine (PZ, CAS No. 110-85-0) and aqueous 2-amino-2-methyl-1-propanol (AMP, CAS No. 124-68-5) were measured. The FPD and solubility were also determined in the ternary AMP–PZ–H₂O system. A method was developed by which solubility can be determined at higher temperatures using the FPD setup. A total of 86 data points are listed in the full concentration range from (–35 to 90) °C. The solid phases piperazine hexahydrate (PZ·6H₂O), piperazine hemihydrate (PZ·1/2H₂O), and anhydrous PZ precipitated during the experiments. The data can be used in the formulation, prevention, or intentional formation of slurries in piperazine solvents for promoting CO₂ capture using absorption and desorption.

1. INTRODUCTION

CO₂ capture is an openly debated topic for carbon emission reduction to reduce pollution by greenhouse gases. Process streams containing carbon dioxide can be cleaned by absorption in aqueous liquid solvents. Amines, strong bases, or combination of the two are typically used as active components. The low heats of absorption and desorption are design criteria that reduce the cost of energy in regeneration of the solvent. This is obtained by using sterically hindered amines. The result is often slow reaction kinetics between the solvent and CO₂. Consequently piperazine (PZ) is being used in solution formulation to create an enhanced CO₂ capture solvent. PZ can be used with both amine and potash solutions (K₂CO₃) to increase the rate of absorption and thereby promote the CO₂ capture.

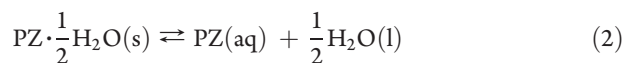
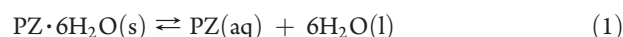
A lower PZ concentration was typically used in literature. Recently the scope has changed, and PZ is now being used at higher concentrations. On increasing the concentration, the solubility limit of PZ is being reached, especially during winter temperatures and even up to room temperature. The unexpected formation of slurries and solids downstream may create unforeseen process conditions, decrease efficiency, and create clogging which will result in unfortunate hazardous operations. In general it could be interesting to provoke the formation of CO₂ containing solids and thereby facilitate and increase the capacity of the capture solvent. CO₂ deprived solids are rarely preferable in terms of CO₂ capture.

The aim of this work is to determine the solid–liquid phase boundary in the two binary PZ–H₂O and AMP–H₂O systems and also in the ternary AMP–PZ–H₂O system. 2-Amino-2-methyl-1-propanol (AMP) is a sterically hindered amine. CO₂ absorption in AMP solutions can be promoted by adding PZ.

An additional goal of this work was to enhance the utilization of freezing-point depression (FPD) equipment developing a method for the purpose of studying solid–liquid equilibrium (SLE) behavior in solutions precipitating solids other than ice.

PZ is a compound which has a variety of applications; for example, it has been used for animal and human intake in the treatment of roundworm infections as an anthelmintic.^{1,2}

The SLE phase boundaries of the aqueous PZ system were examined very early by Berthelot,³ further by Rosso and Carbonnel,⁴ and in summary by Carbonnel and Rosso.⁵ Berthelot³ stated the existence of the hexahydrate PZ·6H₂O, the hemihydrate PZ·1/2H₂O, and possibly a monohydrate. The differential scanning calorimetry (DSC) analysis by Rosso and Carbonnel⁴ confirmed the formation of the following PZ solid hydrate phases, hexahydrate, hemihydrate, and anhydrous PZ with the equilibrium reactions:



Rosso and Carbonnel especially note that the system has two eutectic points, at –1 °C between ice and hexahydrate and at 33 °C between hexahydrate and hemihydrate, including a peritectic point at 58 °C at the intersection between hemihydrate and anhydrous PZ. The hexahydrate melts at 44 °C, and anhydrous PZ melts at 104 °C, as determined by Berthelot,³ Schwarzenbach,⁶ and Rosso and Carbonnel.⁴ A more accurate anhydrous melting point was estimated by Witschonke⁷ of (111.4 and 111) °C by Hetzer et al.,⁸ which is in line with the chemical supplier of this work. Rosso and Carbonnel⁴ present a

Special Issue: Kenneth N. Marsh Festschrift

Received: September 5, 2011

Accepted: November 8, 2011

Published: November 14, 2011

complete SLE phase diagram of the aqueous PZ system with an accuracy of ± 1 °C.

More recently PZ precipitation has received attention during CO₂ capture studies. Bishnoi⁹ and Bishnoi and Rochelle¹⁰ studied SLE by dissolution of the anhydrous PZ until equilibrium, and titration was applied in the analysis of the liquid phase which was repeated by Muhammad et al.¹¹ Hilliard¹² applied a DSC technique similar to Rosso and Carbonnel.⁴

No apparent studies are available on SLE in the binary AMP–H₂O system or in the ternary AMP–PZ–H₂O system.

On the addition of CO₂ the PZ equilibria become very complex. The speciation in the liquid phase will result in a number of new species. Carbonates, bicarbonates, and carbamates are formed. PZ has, opposite MEA (monoethanol amine), the ability to form several different carbamates.^{10,13–15} This is noteworthy in studying PZ systems.

2. EXPERIMENTAL DETAILS

2.1. Materials. White anhydrous PZ was purchased from Fluka at a BioUltra grade, > 99.0 %, and amorphous AMP obtained through Acros at 99 % was used without further purification. The liquid solutions were mixed from the pure chemicals using deionized water with a maximum conductivity of 0.2 μ S.

2.2. Apparatus. The FPDs of the solutions were measured using the apparatus by Fosbøl et al.¹⁶ The solubility measurements were conducted using the SLE titration apparatus described in detail by Fosbøl et al.¹⁷ As outlined below, a new method was developed for which the FPD apparatus could be used for the determination of solubility to obtain results equivalent to the data determined from titration.

2.3. Experimental Method. The freezing point of the solutions was determined using the technique outlined by Fosbøl et al.¹⁶ The SLE behavior for solutions precipitating solids other than ice were analyzed using two methods. The first method performed was the use of a titration setup described by Fosbøl et al.¹⁷ The second method was to determine SLE by the FPD method described below.

The titration results were postprocessed using method III of Fosbøl et al.¹⁸ PZ has two equivalence points similar to titration of aqueous Na₂CO₃ forming PZH⁺ and PZH₂²⁺, and AMP has one, protolysing to AMPH⁺. Seeding the solution by PZ·6H₂O was done for few mixtures which did not precipitate PZ·6H₂O as expected.

SLE by FPD is a new method developed in this study. It builds on the principles of the visual polythermal method. Here a modified Beckman FPD apparatus equivalent to the setup by Fosbøl et al.¹⁶ was used to accurately determine the salt solubility. The apparatus itself was not changed, but the method for determining the phase change was altered. The phase change cannot be recognized the same way Fosbøl et al.¹⁶ described it for ice. The heat developed during phase transition is simply not sufficient to show the same distinct temperature phenomena. This is especially the case for the hydrate precipitation. The reaction rate and the reaction enthalpy need to be reasonably fast and exothermic.

To maintain accuracy, the solubility can be determined by visually inspecting the FPD sample glass while melting the solutions. Initially the solution is cooled until onset of precipitation. The solution is then slowly melted by holding it in air at room temperature while stirring. It can also be lowered into a beaker containing hot water with a temperature higher than the

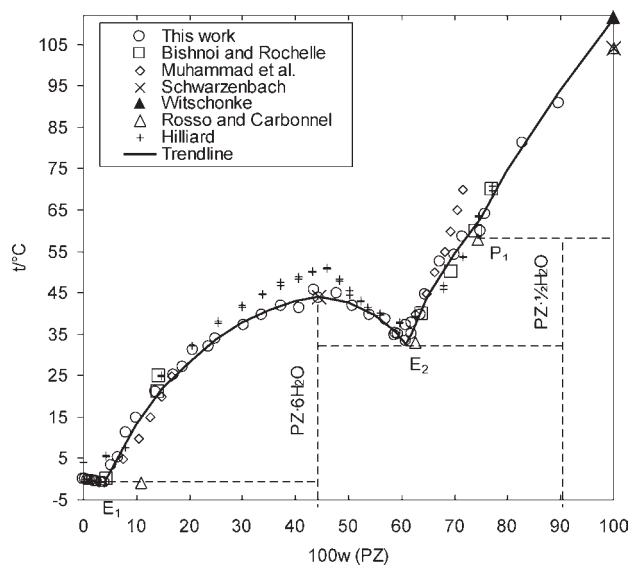


Figure 1. SLE diagram of solid precipitation in the binary PZ–H₂O system as a function of temperature at atmospheric conditions. The line indicates the trend of the data.

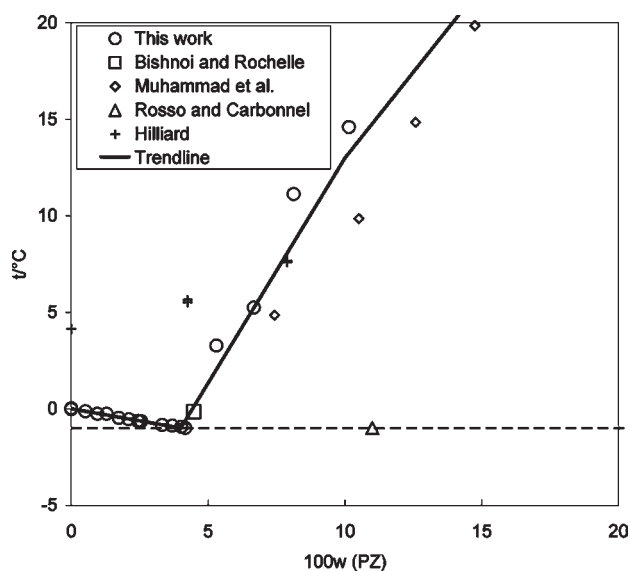


Figure 2. SLE diagram of solid precipitation in the binary PZ–H₂O system for $w(\text{PZ}) < 0.2$ as a function of temperature at atmospheric conditions. The line indicates the trend of the data.

melting point of the mixture. Using the FPD temperature probe, the solubility point is determined by the disappearance of the crystals where the solution becomes clear on heating. A typical accuracy of (0.05 to 0.2) K is obtained using this method. The reproducibility is obtained by consecutively heating and cooling the sample past the solid–liquid phase boundary.

3. RESULTS AND DISCUSSION

The measured solubility data for PZ in water are shown in Figures 1 and 2. Figure 2 focuses on the low concentration range. Solubility data from other studies are also shown in the two figures. The corresponding measurements performed in this work are listed in Table 1. The measured FPD and the solubilities

Table 1. Solubility in the PZ–Water System as a Function of Temperature at Atmospheric Conditions Determined by FPD, SLE by FPD, and Titration Methods

t	$w(\text{PZ})$	σ_t^a	σ_w^a		t	$w(\text{PZ})$	σ_t^a	σ_w^a	
°C	$\text{g} \cdot (\text{g total})^{-1}$	°C	$\text{g} \cdot (\text{g total})^{-1}$	SF ^b	°C	$\text{g} \cdot (\text{g total})^{-1}$	°C	$\text{g} \cdot (\text{g total})^{-1}$	SF ^b
−0.129	0.00521	0.005		ice	41.75	0.3745	0.036		PZ·6H ₂ O
−0.261	0.00953	0.007		ice	41.3	0.409		0.007	PZ·6H ₂ O
−0.259	0.01297	0.01		ice	45.6	0.4356	0.16		PZ·6H ₂ O
−0.467	0.01738	0.002		ice	43.745	0.4437	0.24		PZ·6H ₂ O
−0.543	0.02100	0.003		ice	44.64	0.4782	0.096		PZ·6H ₂ O
−0.629	0.02440	0.004		ice	41.79	0.5093	0.08		PZ·6H ₂ O
−0.626	0.02468	0.007		ice	39.6	0.5396	0.18		PZ·6H ₂ O
−0.639	0.02551	0.011		ice	38.5	0.5699	0.12		PZ·6H ₂ O
−0.845	0.03315	0.006		ice	34.5	0.5885	0.24		PZ·6H ₂ O
−0.876	0.03690	0.024		ice	35.19	0.5903	0.03		PZ·6H ₂ O
−0.931	0.04017	0.011		ice	34.8	0.595		0.005	PZ·6H ₂ O
−0.999	0.04161	0.005		ice	33.4	0.6090		0.0005	PZ·6H ₂ O
3.28	0.0530	0.096		PZ·6H ₂ O	37.03	0.6097	0.06		PZ·1/2H ₂ O
5.25	0.0667		0.0002	PZ·6H ₂ O	37.55	0.619		0.007	PZ·1/2H ₂ O
11.13	0.0812	0.05		PZ·6H ₂ O	34.85	0.619		0.010	PZ·1/2H ₂ O
14.6	0.1015		0.0005	PZ·6H ₂ O	39.6	0.637		0.004	PZ·1/2H ₂ O
20.9	0.1375	0.08		PZ·6H ₂ O	44.5	0.65		0.02	PZ·1/2H ₂ O
25.0	0.1710		0.0009	PZ·6H ₂ O	52.47	0.6720	0.09		PZ·1/2H ₂ O
26.98	0.1884	0.05		PZ·6H ₂ O	54.1	0.70		0.01	PZ·1/2H ₂ O
31.0	0.208		0.01	PZ·6H ₂ O	58.52	0.7153	0.09		PZ
31.94	0.2367	0.06		PZ·6H ₂ O	59.9	0.7494	0.17		PZ
33.88	0.2510	0.05		PZ·6H ₂ O	63.9	0.759		0.006	PZ
37.0	0.304		0.001	PZ·6H ₂ O	81.07	0.8290	0.04		PZ
39.45	0.338		0.01	PZ·6H ₂ O	90.7	0.8977	0.25		PZ

^a Standard deviation of three to five consecutive analyses. ^b Solid-phase type.

from equilibrium analysis using FPD setup and titration are given. The standard deviations of the measurements are shown along with the information of the solid phases.

A repeatability, often better than 0.01 K, was obtained for the FPD analysis, which indicates a good accuracy.

Standard deviations up to 0.2 K were observed for cases using the above SLE by FPD method for concentrations higher than the ice–PZ·6H₂O eutectic point.

A maximum standard deviation of the titration experiments is $\sigma(w(\text{PZ})) = \pm 0.02$ where a typical value is $\sigma(w(\text{PZ})) = \pm 0.001$.

Comparing the two methods of FPD and titration, the qualitative accuracy between experimental points seem to be varying. It is expected that the accuracy is similar to the reproducibility for the cases precipitating ice. For the highly concentrated solutions the accuracy seems to be lower on visually inspecting Figures 1 and 2, possibly in the order of 0.1 K to 1 K and in worst cases up to 2 K where the solubility determination is difficult from an experimental point of view.

3.1. PZ–H₂O System. Figure 1 shows the two eutectic points, E₁ and E₂, in addition to the peritectic point P₁. The trend of the curve is similar to the hydrate formation in a number of inorganic SLE systems. Ice is formed below $w(\text{PZ}) = 0.04$. Amorphous PZ·6H₂O precipitates at $0.04 < w(\text{PZ}) < 0.61$, followed by PZ·1/2H₂O at $0.61 < w(\text{PZ}) < 0.71$, and anhydrous PZ for $w(\text{PZ}) > 0.71$.

Starting up a capture plant at winter type conditions may create difficulties with respect to slurries and clogging using a

piperazine solvent. The diagram in Figure 2 shows that aqueous piperazine freezes completely to solid below -1 °C. Precipitation may even take place at approximately $w(\text{PZ}) = 0.17$ at 25 °C as plotted in Figure 1. An expected local maximum in the solubility is observed by the melting point of PZ·6H₂O. Heating the liquid above 45 °C will cause the dissolution of PZ up to $w(\text{PZ}) = 0.65$, whereas further heating results in a relatively small solubility increase. For concentrations of $w(\text{PZ}) > 0.44$, the solutions become completely solid below 32 °C indicated by the dotted line below E₂ in Figure 1. The solubility points in the vicinity of E₂ at $0.59 < w(\text{PZ}) < 0.65$ are especially difficult to determine. The precipitate makes the solution look like milk with small crystals creeping up the sample container surfaces. It is not fully established whether hemihydrate is in stable equilibrium with the saturated liquid close to concentrations of E₂ or it could be the monohydrate. For $w(\text{PZ}) > 0.65$ hydrous amorphous PZ flakes are formed.

To prevent any solid formation in an aqueous PZ system, it is recommended to keep PZ concentrations low, below $w(\text{PZ}) = 0.04$, and above a temperature of 0 °C.

Figures 1 and 2 include the data of previous works on the aqueous PZ SLE behavior. The initial studies by Berthelot³ and Schwarzenbach⁶ indicated the melting point of PZ hexahydrate to be 44 °C equivalent to this study and the melting point of pure PZ to be 104 °C, even though a more accurate value of 111 °C was published by Witschonke.⁷ The most comprehensive and accurate study was carried out by Rosso and Carbonnel;⁴

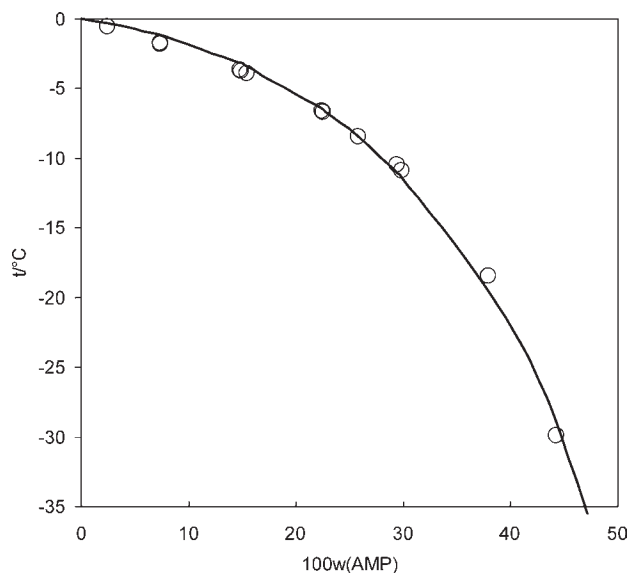


Figure 3. SLE diagram of ice precipitation in the binary AMP–H₂O system as a function of temperature at atmospheric conditions. The line indicates the trend of the data.

unfortunately they only tabulated the eutectic and peritectic points (E_1 , E_2 , P_1) as indicated in the figure. Their original work follows the drawn trend line, except at low PZ concentrations $w(\text{PZ}) < 0.25$. Especially their eutectic point determined at $w(\text{PZ}) = 0.11$ and -1 °C deviates as shown in Figure 2. In this work the eutectic point was determined to be $w(\text{PZ}) = 0.042$ and -1.00 °C.

The work performed by Hilliard¹² deviates at subsections of the SLE boundary compared to the trend line in Figures 1 and 2. This could be due to the critical control needed of the enforced temperature ramp in their used DSC. If a rate too high is used, the measurements may become inaccurate. This is noted by the determined melting point of ice by Hilliard¹² which is 4.16 °C, and the melting point increases while PZ is added. This is unexpected from the thermophysical point of view. Hilliard's data points are approximately 7 K too high for most of the $\text{PZ} \cdot 6\text{H}_2\text{O}$ region compared to the trend line and the measurements of this work and of Schwarzenbach.⁶ On the other hand, the data by Hilliard for $w(\text{PZ}) > 0.52$ resemble the solubilities listed in Table 1. The compositions measured by Bishnoi and Rochelle¹⁰ compare well to the measurements of this work even though the discontinuity they mention does not exist in practice. On the contrary, Muhammad et al.¹¹ listed the solubilities in terms of mole fractions which are not comparable to any of the shown works. By instead converting their measured molarities using the density correlation of Cullinane,¹⁹ the results shown in Figure 1 were obtained. Deviations are observed in most part of the data points, and the curvature is concave whereas a convex trend would be expected.

There is a need for more and accurate experimental data points on the solubility in the complete binary PZ–H₂O system even though the solubility is qualitatively given by Rosso and Carbonnel.⁴ The solubility in the region $w(\text{PZ}) > 0.77$ and below 111 °C is vaguely studied and needs to be further investigated, even though it may be irrelevant for CO₂ capture using this high concentration.

3.2. AMP–H₂O System. The FPD behavior of the binary AMP–H₂O system is shown in Figure 3 for $t > -35$ °C as listed

Table 2. Solubility in the AMP–Water System as a Function of Temperature at Atmospheric Conditions Determined by FPD

t	$w(\text{AMP})$	σ_t^a	
°C	$\text{g} \cdot (\text{g total})^{-1}$	°C	SF ^b
−0.57	0.0249	0.01	ice
−1.86	0.0745	0.02	ice
−1.746	0.0746	0.006	ice
−3.734	0.148	0.004	ice
−3.767	0.1491	0.007	ice
−3.96	0.1553	0.018	ice
−3.92	0.1555	0.016	ice
−6.661	0.2249	0.007	ice
−6.70	0.2257	0.01	ice
−8.49	0.2592	0.02	ice
−10.51	0.2953	0.05	ice
−10.95	0.2992	0.01	ice
−18.53	0.3801	0.09	ice
−30.0	0.4434	0.25	ice

^a Standard deviation of three to five consecutive analyses. ^b Solid-phase type.

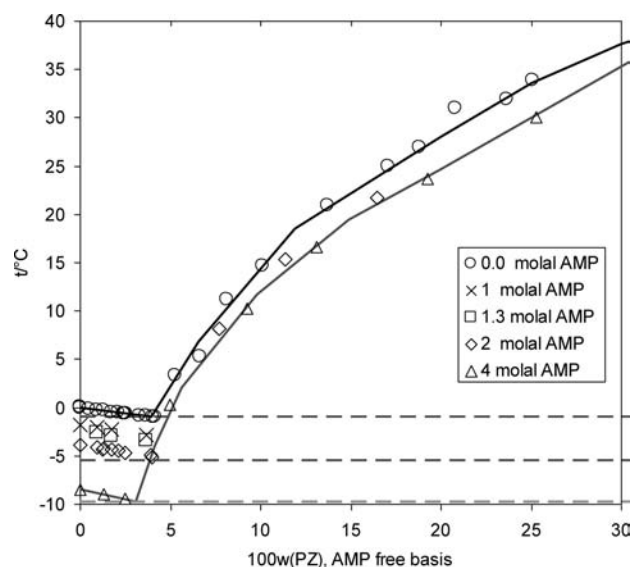


Figure 4. SLE diagram for the ternary AMP–PZ–H₂O system as a function of temperature at atmospheric conditions. Lines indicate the trend of the data for the PZ–H₂O system and the PZ–AMP–H₂O system with 4 *m* AMP.

in Table 2. The table presents the solubilities determined from FPD analysis. In addition, the standard deviations and solid phase information are given. The accuracy is similar to the PZ–H₂O system, giving a standard deviation better than 0.01 K. The concentrated solution for $w(\text{AMP}) > 0.3$ become highly viscous and difficult to stir, which results in lower accuracy of the FPD determination up to 0.2 K in standard deviation.

The phase boundary phenomenon of the AMP–H₂O system is less complicated compared to the aqueous PZ system. There were no indications of hydrate formation at $t > -35$ °C. There is a complete lack of SLE data for comparison, and there is a need

Table 3. Solubility in the Ternary AMP–PZ–Water System as a Function of Temperature at Atmospheric Conditions Determined by FPD and the SLE by FPD Methods

t	$w(\text{AMP})$	$w(\text{PZ})$	σ_f^a		t	$w(\text{AMP})$	$w(\text{PZ})$	σ_f^a	
°C	$\text{g} \cdot (\text{g total})^{-1}$	$\text{g} \cdot (\text{g total})^{-1}$	°C	SF ^b	°C	$\text{g} \cdot (\text{g total})^{-1}$	$\text{g} \cdot (\text{g total})^{-1}$	°C	SF ^b
−2.011	0.0754	0.00881	0.006	ice	−4.874	0.1503	0.0332	0.007	ice
−2.246	0.0784	0.0160	0.006	ice	−5.11	0.1501	0.0337	0.018	ice
−2.80	0.0790	0.0340	0.015	ice	8.2	0.1453	0.0659	0.16	PZ·6H ₂ O
−2.58	0.0975	0.00860	0.013	ice	15.3	0.1403	0.0980	0.17	PZ·6H ₂ O
−2.88	0.1009	0.0156	0.01	ice	21.7	0.1333	0.1425	0.21	PZ·6H ₂ O
−3.36	0.1000	0.0332	0.02	ice	−8.98	0.2567	0.00958	0.023	ice
−4.086	0.1484	0.00812	0.005	ice	−9.45	0.2543	0.0185	0.017	ice
−4.311	0.1537	0.0107	0.009	ice	0.25	0.2494	0.0375	0.057	ice
−4.24	0.1538	0.0108	0.014	ice	10.237	0.2410	0.0702		PZ·6H ₂ O
−4.293	0.1477	0.0148	0.007	ice	16.658	0.2331	0.1007	0.006	PZ·6H ₂ O
−4.47	0.1528	0.0177	0.027	ice	23.65	0.2203	0.1501	0.01	PZ·6H ₂ O
−4.67	0.1521	0.0208	0.01	ice	30.0	0.2073	0.2002	0.09	PZ·6H ₂ O

^a Standard deviation of three to five consecutive analyses. ^b Solid-phase type.

for detailed DSC analysis of the complete phase boundary. The solubility was not measured below -35 °C due to limitations by the used ice bath.

3.3. AMP–PZ–H₂O System. The freezing points of the ternary mixtures are shown in Figure 4 as laid out in Table 3. The information given is in accordance with Tables 1 and 2. The SLE curve of the binary PZ–H₂O system corresponding to Figure 2 is included in this figure. The effect of the addition of AMP is marked by the consecutive series of data for $b(\text{AMP}) = (1.0, 1.3, 2.0, \text{ and } 4.0) \text{ mol AMP} \cdot \text{kg}^{-1} \text{ H}_2\text{O}$. The freezing points of the solutions decrease on addition of AMP. At $b(\text{AMP}) = 2.0 \text{ mol AMP} \cdot \text{kg}^{-1} \text{ H}_2\text{O}$ the FPD of AMP in aqueous PZ is approximately (4.1 and 8.5) K at $b(\text{AMP}) = 4.0$. AMP and PZ have an observed and expected effect similar to the MEA and MDEA¹⁶ whereby both chemicals induce FPD in the aqueous system. The recommendations for avoiding precipitation in the ternary system are equivalent to those for the aqueous PZ system as discussed above. Solid formation may only be completely prevented by using PZ concentrations below $w(\text{PZ}) < 0.04$ above 0 °C. There is a need for additional experimental data to perform a comparison for the reproducibility of the measured data since no other works are available. Further, measurements of solubility in highly concentrated solutions above a $w(\text{PZ}, \text{AMP free}) = 0.25$ concentration are needed.

Thermodynamic modeling is currently being done in a more intensive study on PZ phase equilibria.

4. CONCLUSION

In this work the solubility in aqueous PZ, AMP, and PZ–AMP systems was determined by freezing-point measurements and by titration. An additional new method for solubility determination based on the visual polythermal approach was developed and applied in this work. This method can be called SLE by FPD. It extends freezing-point determination to other solids than ice.

A total of 86 new data points were determined in the temperature range (-35 to 90) °C. This was done with the intention to study precipitation and slurry formation in relation to carbon capture and sequestration. This type of studies is relevant for the reduction of greenhouse gas emissions. The data

were measured to improve the basis for thermodynamic modeling of the system. There is a general lack of this type of data in the literature; further analyses of the SLE phenomenon in these systems are needed.

The effect of CO₂ loading may contribute to the formation of solids in the system, and it is important to be aware of the possible effects by dissolved CO₂. In this work the unloaded solvent was studied to identify a safe range of solvent concentrations for formulation and handling.

■ AUTHOR INFORMATION

Corresponding Author

*Tel.: +45 4525 2800. Fax: +45 4588 2258. E-mail address: plf@kt.dtu.dk.

Funding Sources

We acknowledge the valuable consortium funding to the Center for Energy Resources Engineering (CERE) enabling the maintenance of an efficient lab at CERE.

■ REFERENCES

- (1) FDA. Oral dosage from new animal drugs; piperazine. *Fed. Regist.* **1999**, *64* (82), 23017–23019.
- (2) Bellander, T.; Osterdahl, B. G.; Hagmar, L. Formation of N-mononitrosopiperazine in the stomach and its excretion in the urine after oral intake of piperazine. *Toxicol. Appl. Pharmacol.* **1985**, *80* (2), 193–8.
- (3) Berthelot, M. Investigations over the Diamines: Diethyl Diamine (Piperazine). *C. R. Hebdomad. Seances Acad. Sci.* **1899**, *129*, 687–94.
- (4) Rosso, J. C.; Carbonnel, L. Water-Piperazine System. *C. R. Hebdomad. Seances Acad. Sci., Ser. C* **1974**, *278* (5), 307–309.
- (5) Carbonnel, L.; Rosso, J. C. New Nitrogen Heterocycles Crystallizing as Cubic Clathrate Hydrates. Stoichiometry of the New Phases as Deduced from the Water-Heterocycle Phase Diagrams. *Bull. Soc. Chim. Fr.* **1976**, 7–8 (Pt. 1), 1043–50.
- (6) Schwarzenbach, D. Structure of Piperazine Hexahydrate. *J. Chem. Phys.* **1968**, *48* (9), 4134–4140.
- (7) Witschonke, C. R. Freezing Point and Purity Data for Some Organic Compounds. *Anal. Chem.* **1954**, *26* (3), 562.
- (8) Hetzer, H. B.; Robinson, R. A.; Bates, R. G. Dissociation Constants of Piperazinium Ion and Related Thermodynamic Quantities from 0 to 50 °C. *J. Phys. Chem.* **1968**, *72* (6), 2081–2086.

(9) Bishnoi, S. *Carbon Dioxide Absorption and Solution Equilibrium in Piperazine Activated Methyl-diethanolamine*. Ph.D. Dissertation, University of Texas, Austin, TX, 2000.

(10) Bishnoi, S.; Rochelle, G. T. Thermodynamics of Piperazine/Methyl-diethanolamine/Water/Carbon Dioxide. *Ind. Eng. Chem. Res.* **2002**, *41* (3), 604–612.

(11) Muhammad, A.; Abdul Mutalib, M. I.; Murugesan, T.; Shafeeq, A. Thermophysical Properties of Aqueous Piperazine and Aqueous (N-Methyl-diethanolamine + Piperazine) Solutions at Temperatures (298.15 to 338.15) K. *J. Chem. Eng. Data* **2009**, *54*, 2317–2321.

(12) Hilliard, M. A. *Predictive Thermodynamic Model for an Aqueous Blend of Potassium Carbonate, Piperazine, and Monoethanolamine for Carbon Dioxide Capture from Flue Gas*. Ph.D. Dissertation, University of Texas, Austin, TX, 2008.

(13) Bishnoi, S.; Rochelle, G. T. Absorption of Carbon Dioxide into Aqueous Piperazine: Reaction Kinetics, Mass Transfer and Solubility. *Chem. Eng. Sci.* **2000**, *55*, 5531–5543.

(14) Bishnoi, S.; Rochelle, G. T. Absorption of Carbon Dioxide in Aqueous Piperazine/ Methyl-diethanolamine. *AIChE J.* **2002**, *48* (12), 2788–2799.

(15) Ermatchkov, V.; Pérez-Salado Kamps, Á.; Maurer, G. Chemical Equilibrium Constants for the Formation of Carbamates in (Carbon Dioxide + Piperazine + Water) from ¹H-NMR-Spectroscopy. *J. Chem. Thermodyn.* **2003**, *35* (8), 1277–1289.

(16) Fosbøl, P. L.; Pedersen, M. G.; Thomsen, K. Freezing Point Depressions of Aqueous MEA, MDEA, and MEA-MDEA Measured with a New Apparatus. *J. Chem. Eng. Data* **2011**, *56*, 995–1000.

(17) Fosbøl, P. L.; Thomsen, K.; Stenby, E. H. Solubility Measurements in the Mixed Solvent Electrolyte System Na₂CO₃-NaHCO₃-Monoethylene Glycol-Water. *Ind. Eng. Chem. Res.* **2009**, *48* (4), 2218–2228.

(18) Fosbøl, P. L.; Thomsen, K.; Stenby, E. H. Reverse Schreinemakers Method for Experimental Analysis of Mixed-Solvent Electrolyte Systems. *J. Solution Chem.* **2009**, *38* (1), 1–14.

(19) Cullinane, J. T. *Carbon Dioxide Absorption in Aqueous Mixtures of Potassium Carbonate and Piperazine*. M.S. Thesis, University of Texas, Austin, TX, 2002.